applied sciences

MDPI

Article

Effect of Mother's Age and Pathology on Functional Behavior of Amniotic Mesenchymal Stromal Cells—Hints for Bone Regeneration

Maria Matteo [1], Elisa Beccia [2,*], Annalucia Carbone [3], Stefano Castellani [1], Lucio Milillo [4], Dorina Lauritano [5], Sante Di Gioia [1], Antonella Angiolillo [2] and Massimo Conese [1,*]

1 Department of Medical and Surgical Sciences, University of Foggia, 71122 Foggia, Italy
2 Department of Medicine and Health Sciences "V. Tiberio", University of Molise, 86100 Campobasso, Italy
3 Division of Internal Medicine and Chronobiology Unit, IRCCS "Casa Sollievo della Sofferenza", 71013 San Giovanni Rotondo, Italy
4 EOS IMPLANT, 70124 Bari, Italy
5 School of Medicine and Surgery, University of Milano-Bicocca, 20900 Monza, Italy
* Correspondence: e.beccia@studenti.unimol.it (E.B.); massimo.conese@unifg.it (M.C.); Tel.: +39-0881-588019 (M.C.)

Received: 25 July 2019; Accepted: 20 August 2019; Published: 22 August 2019

Featured Application: The amnion, obtained at parturition, is an ethical and abundant source of mesenchymal stromal cells with stem cell-like properties useful for application to dentistry, The exact knowledge of the interaction of amnion-derived stromal cells with titanium surfaces will bring forth the production of dental implants with optimized and long-term characteristics of osteoinduction and osseointegration.

Abstract: Human amnion-derived mesenchymal stromal cells (hAMSCs) are used increasingly in regenerative medicine applications, including dentistry. The aim of this study was to evaluate if hAMSCs from aged and pathological mothers could be affected in their phenotype and functional behavior. hAMSCs were isolated from placentas of women aged younger than 40 years (Group 1, n = 7), older than 40 years (Group 2, n = 6), and with pre-eclampsia (Group 3, n = 5). Cell yield and viability were assessed at isolation (p0). Cell proliferation was evaluated from p0 to p5. Passage 2 was used to determine the phenotype, the differentiation capacity, and the adhesion to machined and sandblasted titanium disks. hAMSCs recovered from Group 3 were fewer than in Group 1. Viability and doubling time were not different among the three groups. Percentages of $CD29^+$ cells were significantly lower in Group 3, while percentages of $CD73^+$ cells were significantly lower in Groups 2 and 3 as compared with Group 1. hAMSCs from Group 2 showed a significant lower differentiation capacity towards chondrogenic and osteogenic lineages. hAMSCs from Group 3 adhered less to titanium surfaces. In conclusion, pathology can affect hAMSCs in phenotype and functional behavior and may alter bone regeneration capacities.

Keywords: amnion; mesenchymal stem cells; pre-eclampsia; differentiation; adhesion; titanium

1. Introduction

Regenerative medicine in dentistry is applied in biotooth/bioroot engineering, regeneration of periodontal defects, and dentin-pulp regeneration strategies [1] by using a combination of scaffold, growth factors, and stem cells [2]. Within such context, polymers and commercially pure titanium membranes are used for dental implants and orthopedic surgery as scaffolds for engendering endogenous cells' proliferation and migration, however they are bioinert materials that do not

stimulate bone formation (i.e., they are not osteoinductive) and do not directly bond to bone [3]. This is why titanium surfaces, most commonly used in dental implants, have been engineered to determine the appropriate scaffold properties (e.g., porosity, surface geometry, and mechanical strength) in order to support the necessary cell activity to promote bone regrowth by the host cells [4].

Among the cell types used for bone regenerative purposes, stem cells are considered more than a promising strategy to achieve the regeneration of large alveolar bone defects, particularly to provide stable and accelerated bone formation as well as enhanced osseointegration in dental implant treatments. Mesenchymal stem cells (MSCs) have been identified as a significant cell source for regenerative medicine due to their self-renewal, easy growth in vitro that allows them to expand, their differentiation capacities, and immunomodulatory properties [5]. Although MSCs are classically derived from the bone marrow (BM), other sources are, among the others, many tissues in the orofacial region, the adipose tissue, and the placental tissue. The application of MSCs derived from the amniotic membrane is increasingly recognized as a therapeutic option for the purposes of regenerative medicine and tissue engineering, because of the easiness of their acquisition, reduced donor damage, multipotency, low immune response, and acceptable ethical issue [6]. Human amniotic mesenchymal stromal cells (hAMSCs) have stem cell-like properties and are able to differentiate into cells derivable from each of the three germ layers, including osteogenic, chondrogenic, and adipogenic lineages [7–11]. Similar to BM-MSCs, hAMSCs express typical mesenchymal antigens such as CD29, CD73, and CD105 and lack hematopoietic markers CD34, CD45, and CD14. The application of hAMSCs to tissue engineering and cell replacement studies has shown their therapeutic potential in different clinical fields, including dentistry, orthopedics, skin reconstruction, as well as in liver, cardiac, and respiratory diseases [12–14].

A limit in using MSCs derived from the classical source, i.e., the BM, is their dependence on donors [15]. The number of BM-MSCs declines with age, as well as their fitness, explored as an increase in reactive oxygen species and oxidative stress, is reduced with ageing [16]. Another study demonstrated an age-dependent reduction in the proliferation and differentiative capacity towards the osteoblast lineage in BM-MSCs [17]. Also, the disease state may affect the collection of sufficient healthy autologous BM for transplantation, as well as their functionality [18–20].

Since no studies have been carried out to reveal if hAMSCs features can be modified by age and pathology, we have undertaken a study to ascertain whether mother's age and pre-eclampsia (PE) can affect the functional behavior of hAMSCs. We have chosen PE since it is a relatively common pregnancy disorder that may threaten the survival of both mother and baby [21]. Some evidence highlighted that PE is a systemic vascular disorder whose hallmark is a disturbed angiogenic balance [22]. Our findings show that hAMSCs are affected by age and PE, in particular PE affects their adhesion to titanium surfaces, implying that PE hAMSCs may be not osteoconductive when used in combination with titanium-based dental implants.

2. Materials and Methods

2.1. hAMSC Isolation

Human placentas from Group 1 (<40 years of maternal age), Group 2 (more than 40 years of maternal age), and Group 3 (pre-eclamptic) pregnancies were collected and processed immediately [23]. Pre-eclamptic placentas were selected according to the National High Blood Pressure Education Program Working Group on High Blood Pressure in Pregnancy and the American College of Obstetricians and Gynecologists and Task Force on Hypertension in Pregnancy [24]: hypertension ≥140/90 mmHg on ≥2 occasions at least 4 h apart in a woman who was normotensive before the 20th week of gestation with proteinuria ≥300 mg/24 h. Women belonging to the three Groups were Caucasian, were nonsmokers and had not consumed alcohol, had no diabetes or other comorbidities, and had not received prenatal medications. Delivery through Caesarean section was performed in: n = 6 Group 1 (86%), n = 2 Group

2 (33%), and n = 1 Group 3 (20%). In all cases enrolled, the third stage of labor was physiological and the delivery of placenta occurred within 20 min.

Human amniotic mesenchymal stromal cells were isolated, as previously described [25], from a piece of amniotic membrane (AM) of 5 cm^2. The yield is then the number of cells retrieved for each specimen. The viability of retrieved cells was evaluated by the trypan blue exclusion test.

Informed consent was obtained from all women for being included in the study. The study was conducted in accordance with the Declaration of Helsinki, and the protocol was approved by the Ethics Committee of the Ospedali Riuniti of Foggia (Project identification code 68/19).

2.2. hAMSC Growth and Phenotype Analysis

Freshly isolated (p0) hAMSCs were subcultured until passage 5 (p5) by plating at a density of $1 \times 10^5/cm^2$ in Advanced DMEM (Gibco, Life Technologies Limited, Paisley, UK) supplemented with 10% (v/v) fetal bovine serum (FBS), 55 µM β-mercaptoethanol, 1% di L-glutamine, 1% penicillin/streptomycin (Invitrogen, Milan, Italy), and 10 ng/mL epidermal growth factor (EGF; Sigma). Every time cells reached 80% of confluence, cells were detached with trypsin-ethylendiaminetetracetic acid (EDTA) (Invitrogen, Thermo Fisher Scientific, Monza, Italy), washed, counted with a Bürker chamber, and replated in a new T25 plastic flask at a density of 5×10^5 in order to calculate their growth curve. Doubling time was calculated, inserting times and cell counts on the website http://www.doubling-time.com/compute.php.

For phenotypic analysis, cells were then stained with fluorochrome-conjugated monoclonal antibodies against hematopoietic (CD14, CD34, CD45) or mesenchymal (CD29, CD73, CD105) markers, as previously published [25]. All antibodies were purchased from Invitrogen, ThermoFisher Scientific (Waltham, MA, USA), and were conjugated with fluorescein isothiocyanate (FITC), except the antibody against CD73 that required an additive incubation with secondary antibody (FITC goat anti-mouse; Sigma-Aldrich, Milan, Italy) for 30 min at 4 °C. At least, 1×10^6 cells were finally analyzed using the Amnis Flowsight IS100 (Merck KGaA, Darmstadt, Germany). Negative controls included FITC-conjugated isotype antibodies (IgG1 kappa, Invitrogen), FITC-conjugated goat anti-mouse in the absence of the primary antibody for CD73 analysis, no antibody, or unconjugated goat anti-mouse antibody.

Analysis of positive cells was obtained with the IDEAS 6.0 Software (Amnis, EMD Millipore, Seattle, WA, USA). Cells in best focus, i.e., those with higher Gradient root mean square (RMS) values, were chosen. Brightfield scatter plots obtained by plotting Area (a parameter relative to cellular dimension) on x-axis vs. Aspect Ratio (a parameter reflecting the ratio of the cell Minor Axis divided by the Major Axis) on y-axis were generated to identify single cells events, i.e., those with an intermediate Area value and a high Aspect Ratio. The intensity of Ch02 (FITC fluorescence channel) vs. normalized frequency was used to calculate the statistics Count and Percent Gated on 10,000 single-cell events for sample.

At p0 and p2, before phenotypic analysis, cells images were taken using the inverted microscope (Leica DMRB, Leica Microsystems, Wetzlar and Mannheim, Germany) and captured by the digital camera Leica DFC450 C.

2.3. Differentiation of hAMSCs

2.3.1. Osteogenic Differentiation

In order to induce osteogenesis, hAMSCs at p2 were harvested and plated on cell culture plate at the number of 5×10^4 in a 6 well plate for each well. Cells were then induced for four weeks with osteogenic medium: DMEM high glucose supplemented with 2% FBS, 1% antibiotic solution, 50 µg/mL ascorbate-2-phosphate, 10^{-8} M dexamethasone, 10^{-2} M β-glicerophosphate. The presence of calcium deposits in induced cultures was determined by Alizarin Red (Sigma-Aldrich) staining, as previously published [26].

2.3.2. Chondrogenic Differentiation

In order to evaluate the chondrogenetic potential, hAMSCs at p2 were harvested and plated on cell culture plate at a number of 5×10^4 in a 6 well plate for each well. Cells were then maintained for four weeks in chondrogenic induction medium: DMEM low glucose supplemented with 1% FBS, 1% antibiotic solution, 6.25 µg/mL insulin, 10 ng/mL TGF-β3, 50 nM ascobate-2-phosphate. The presence of proteoglycans in induced cultures was determined by Safranin O (Sigma) staining, as previously published [26].

All cultures were observed at the inverted microscope (Leica DMRB) and captured by the digital camera Leica DFC450 C.

Images were taken from each culture condition in double, considering 10X fields. In order to perform analysis of differentiation into the two mesenchymal lineages, jpeg image files of samples were accessed in Photoshop 7.0 (Adobe, San Jose, CA, USA). Each image was divided into three parts, and each of them was first analyzed for the total number of pixels by accessing Image > Histogram. Then, the same part was accessed in Select > Color range and analyzed for number of pixels corresponding to stained cells, and subsequently by Image > Histogram. The pixel ratio for each image was calculated by dividing the stained number of pixels by the total number of pixels. For each culture condition, hAMSCs from three donors for each Group were used.

2.4. Adhesion to Titanium Disks

Titanium disks were 6 mm diameter and 2.5 mm in height and were prepared from grade 4 unalloyed ISO 5832/2 titanium rods (EOS Implant SRLS, Bari, Italy). Disks had two different titanium surfaces, machined (smooth) or sandblasted. Sandblasted titanium disks were prepared by sandblasting with 100 mesh ultrapure Al_2O_3. The roughness of the sandblasted surface was quantified using a rugosimeter (Talysurf CCI 3000, Taylor Hobson, Milan, Italy) giving a mean surface roughness (Sa) value of 1.5 µm. The surface profile of sandblasted disks was determined using the software Talymap 3D (Taylor Hobson, Milan, Italy).

hAMSCs were labeled with chloromethylbenzamido (CellTracker CM-Dil; Invitrogen), as previously published [25]. Briefly, cells grown at confluence in a T25 flask were washed with phosphate-buffered saline (PBS) and then incubated with the dye working solution (0.0025 ng/µL in DMSO) for 30 min at 37 °C. After labelling, cells were washed twice with PBS, then detached and plated 1.5×10^5 for each disk. Disks were placed into a 48 well plate and incubated at 37 °C 5% CO_2 for 3, 6, 24, 48, and 72 h. At each time point, fluorescence (excitation 553 nm; emission 570 nm) was evaluated at the FilterMax F5 Multi-Mode Microplate Reader (Molecular Devices, Beckman Coulter, Brea, CA, USA). In order to avoid interference of titanium opacity in the path towards the instrument detector, the "top reading" modality was used. The fluorescence was read by well scan method (well scan setting: fill; points per well: 52; density: 8; point spacing: 0.8 mm) using the SoftMax Pro 6.3 (Molecular Devices, Sunnyvale, CA, USA). Fluorescence obtained from unstained cells was subtracted from that obtained with stained cells. The resulting fluorescence was expressed in arbitrary units (A.U.).

2.5. Statistical Analysis

Due to low numbers of donors in the three Groups, Kruskall–Wallis with Dunn's post hoc test was used for parameters such as mother's age, gestational age, child's weight, yield, viability, doubling time, phenotypic, and differentiation analysis. For adhesion to titanium disks, where three experiments were carried out, comparisons between groups were made using ANOVA and Tukey's post hoc test. Data were analyzed by using Prism 5 (Graph-Pad Software, Inc., La Jolla, CA, USA). Differences were considered significant at 95% level of confidence ($P < 0.05$).

3. Results

3.1. Characteristics of Donors

Clinical characteristics of pregnancies for placentas studied are presented in Table 1. Women belonging to Group 3 (pre-eclamptic) had a gestational age significantly shorter than the expectants in Group 2 (mother's age > 40 years). Also, the child's weight was lower in group 3 as compared with the other Groups, although not significantly.

Table 1. Characteristics of pregnancies considered in this study.

Study Group	Mother's Age (years)	Gestational Age (weeks)	Newborn Sex	Child Weight (gr)
Group 1 <40 years (n = 7)	28.7 ± 6.7	39.6 ± 1.1	M =4 F = 3	3327 ± 468
Group 2 >40 years (n = 6)	41.8 ± 2.0 **	40.3 ± 0.9	M = 3 F = 3	3375 ± 185
Group 3 Pre-eclampsia (n = 5)	30.6 ± 2.4 *	37.3 ± 2.2 *	M = 3 F = 2	2740 ± 439

Data are shown as mean ± S.D. ** $P < 0.01$ mother's age Group 2 vs. Groups 1; * $P < 0.05$ mother's age Group 3 vs. Group 2; * $P < 0.05$ gestational age Group 3 vs. Group 2.

3.2. Age and Pathology Affect Hamsc Yield, Viability, and Cell Proliferation

The number of cells isolated from each AM and the percentage of viable cells was not different between Group 2 and Group 1 (Figure 1A,B). Group 3 yielded significantly fewer cells than Group 1, although they were similarly viable (Figure 1A,B). In general and for all hAMSC populations, cell proliferation declined beyond passage two, but was slower for Groups 2 and 3. In the Group 1, in the exponential growth phase, hAMSCs presented a median doubling time of 16.3 days, calculated over five passages. The doubling time was longer for Groups 2 and 3 (medians of 21.4 and 22.1 days, respectively) as compared with Group 1, but not significantly (Figure 1C).

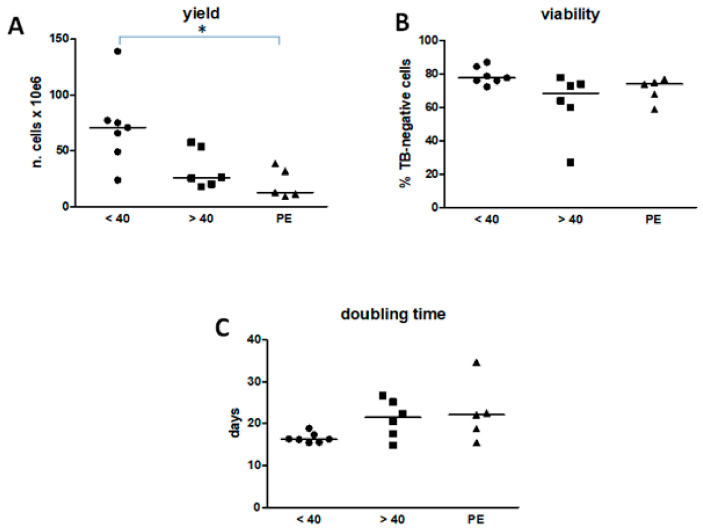

Figure 1. Yield, viability and doubling time of human amnion-derived mesenchymal stromal cells (hAMSCs). (**A**) The yield refers to the same area of amniotic membrane (5 cm^2) for each group. (**B**) The viability refers to the percentage of cells which have excluded the trypan blue (TB). (**C**) The doubling time refers to cells grown from p0 to p5. In (A) * $P < 0.05$ of Group 3 vs. Group 1. Results are shown as individual values and median as a straight line, within each Group (Group 1, n = 7; Group 2, n = 6; Group 3, n = 5).

3.3. hAMSC Marker Expression is Modified by Age and Pathology

At isolation and during passaging, hAMSCs were characterized by a spindle-shape, elongated morphology and adherence to plastic, and could be kept in culture until passage 5 without any change in morphology. Figure S1 shows that the morphology and size of hAMSCs belonging to the three Groups at p0 and p2 were very similar.

An imaging-based flow cytometry apparatus was used to gate cells in best focus, select single cells, and determine the fluorescence intensity on the selected population of cell markers identifying mesenchymal stem cells (CD29, CD73, and CD105). Figure 2 shows representative panels of the analysis carried out on the Group 1 at p2. In Panel C, ten cells for each condition are shown as different channels: brightfield, FITC fluorescence, and side scatter. The same analysis was done with hAMSCs obtained from Groups 2 and 3 (not shown).

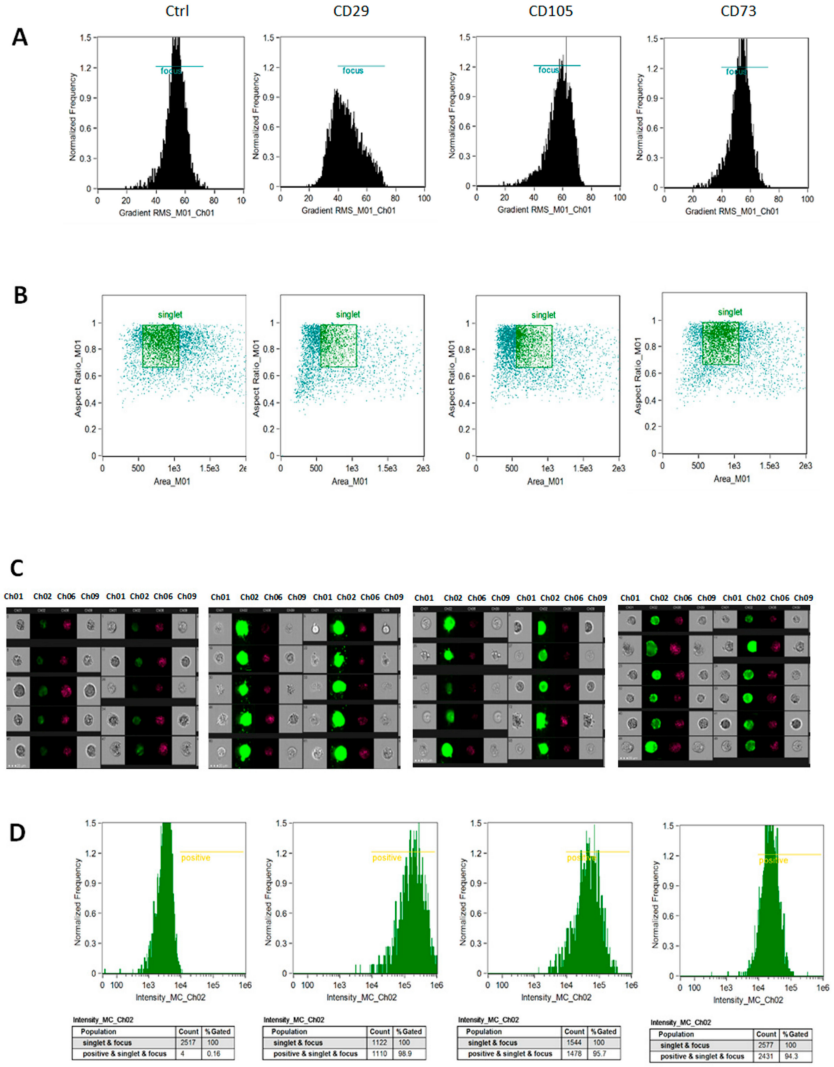

Figure 2. Strategy of flow cytometric analysis for hAMSC phenotypic markers. Cells in best focus, i.e., those with higher Gradient root mean square (RMS) values, were identified (**A**) to draw brightfield scatter plots, (**B**) obtained by plotting Area vs. Aspect Ratio, to identify single cells events (identified by a square region). In (**C**), ten cells for condition are shown, five on the first four columns and five more on the last four columns, as different channels: Ch01 and Ch09 (brightfield); Ch02 (FITC fluorescence); Ch06 (side scatter). The intensity of Ch02 vs. normalized frequency (**D**) was used to calculate the statistics Count and Percent Gated on 10,000 single-cell events for sample. Ctrl = cells incubated in the absence of antibody. The analysis for p2 hAMSCs of Group 1 is depicted. FITC: fluorescein isothiocyanate.

Using this strategy, we obtained that CD29 was expressed at lower levels of Group 3 in comparison with cells obtained from Group 1 (Figure 3A). No significant changes were found for CD105 (Figure 3B). On the other hand, CD73 expression was significantly decreased in Groups 2 and 3 both compared with Group 1 (Figure 3C).

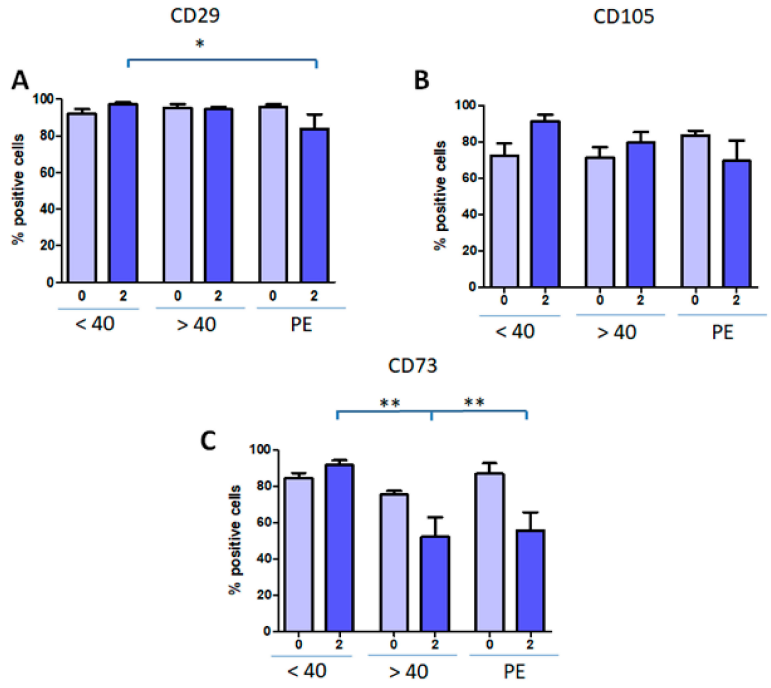

Figure 3. Mesenchymal marker expression in hAMSCs from all Groups. hAMSCs were evaluated for CD29 (**A**), CD105 (**B**), CD73 (**C**) markers at isolation (p0) and p2 by flow cytometry. Results are expressed as mean ± SD of triplicates for each isolate (Group 1, n = 7; Group 2, n = 6; Group 3, n = 5). * $P < 0.05$; ** $P < 0.01$.

The same cytofluorimetric strategy was used for hematopoietic markers (not shown). From the isolation to the p2, the expression of CD14, CD34, and CD45 was negligible for all the hAMSCs from the three Groups, as expected for mesenchymal stem cells (Table 2). These results reproduce well those we have found in an earlier work on hAMSCs obtained from another cohort of women (n = 3), in which we showed at p0 and p2 negligible to null expression of hematopietic markers, high expression of CD29 (p0 range: 66–86%; p2 range: 95–99%) and CD73 (p0 range: 88–91%; p2 range: 88–99%), and lower expression of CD105 (p0 range: 30–66%; p2 range: 40–76%) [25].

Table 2. Hematopoietic markers of hAMSCs belonging to the three study groups.

Study Group	CD14	CD34	CD45
Group 1 (<40)			
p0	3.4 ± 1.2	3.4 ± 1.9	3.9 ± 2.5
p2	2.9 ± 1.3	3.6 ± 1.7	3.8 ± 2.0
Group 2 (>40)			
p0	0.8 ± 0.3	0.6 ± 0.7	0.9 ± 1.0
p2	2.8 ± 1.6	0.9 ± 0.6	1.8 ± 1.8
Group 3 (PE)			
p0	0.8 ± 0.4	1.3 ± 0.2	2.1 ± 1.4
p2	1.5 ± 1.2	1.0 ± 0.2	2.0 ± 1.5

Values are shown as percentages of positive cells and expressed as mean ± SD of triplicates for each isolate.

3.4. Differentiation Capacity of hAMSCs

The differentiation of hAMSCs was tested by evaluating their capacity to give rise to osteogenic and chondrogenic lineages upon culture in specific differentiation media. The analysis of differentiation was carried out on p2 and after 4 weeks of induction, and evidenced by cytochemistry techniques. Staining with Alizarin Red showed that Group 1 hAMSCs presented a clear and robust differentiation towards the osteogenic lineage. hAMSCs induced in the chondrocytic medium were characterized by the formation of typical cellular aggregates that stained with Saphranin O (Figure 4A).

hAMSCs from Group 2 denoted osteogenic differentiation capacity, and also showed differentiation towards the chrondrogenic lineage, as shown by the positive staining of cell aggregates, although these differentiation capacities appeared to be lower than those for Group 1 (Figure 4A).

Similar results were obtained with hAMSCs belonging to Group 3, i.e., the differentiation towards osteogenic and chondrogenic lineages was observed by morphological changes and positive staining for calcium deposits and proteoglycans, respectively, with lower stainings in comparison with Group 1 (Figure 4A).

Image analysis determined that hAMSCs from Group 2 were characterized by a lower differentiation capacity towards osteogenic and chrondrogenic lineages in comparison with Group 1, while Group 3 hAMSCs showed a nonsignificant tendency to lower differentiation capacities (Figure 4B).

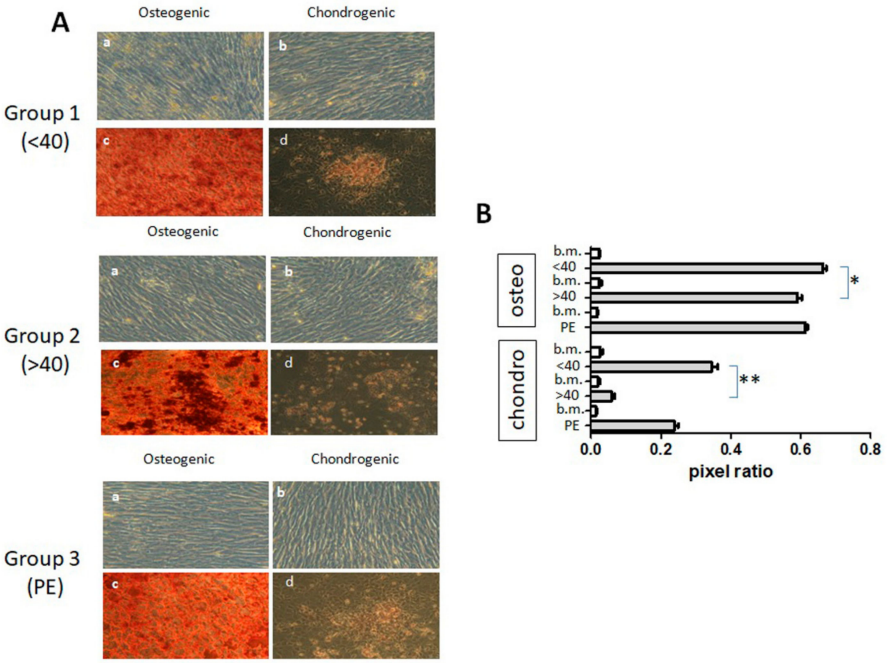

Figure 4. Differentiation of hAMSCs obtained from Group 1, Group 2, and Group 3. Panel (**A**) shows p2 cells that were induced either in basal medium (a, b) or in differentiation medium of osteogenesis (c) or chondrogenesis (d). Representative panels of three different hAMSC isolates for each Group are shown. Magnification: 10×. Panel (**B**) illustrates the pixel ratio of hAMSCs of the three donors for each Group grown in different conditions. b.m. stands for basal medium (conditions a and b in Panel A). * $P < 0.05$; ** $P < 0.01$.

3.5. Pre-Eclampsia Affects hAMSCs Adhesion

The strong induction of osteogenic differentiation prompted us to evaluate the adhesion of hAMSCs onto titanium surfaces that could be used in dentistry for osteoinduction. Since cell responses in terms of adhesion and growth can vary accordingly with different rugosity of titanium [27], two different surfaces were evaluated. In Figure 5A, a three-dimensional view of sandblasted disk surface profile is shown. CM-DiL-labelled hAMSCs from Group 1 adhered to either machined (smooth) or sandblasted

disks with no statistically significant differences (Figure 5B). There was also an increase in the signal associated with cells, however only with the sandblasted disks it was possible to observe a significant increase in cell-associated fluorescence over time. hAMSCs from Group 2 showed similar fluorescence intensity associated with cells to that of hAMSCs from Group 1, with both titanium surfaces (Figure 5B). The sandblasted surface allowed an increase in cell-associated fluorescence of Group 2 hAMSCs with time, but with no statistically significant differences. On the other hand, Group 3 hAMSCs adhered considerably less in comparison with cells from Groups 1 and 2 (Figure 5B).

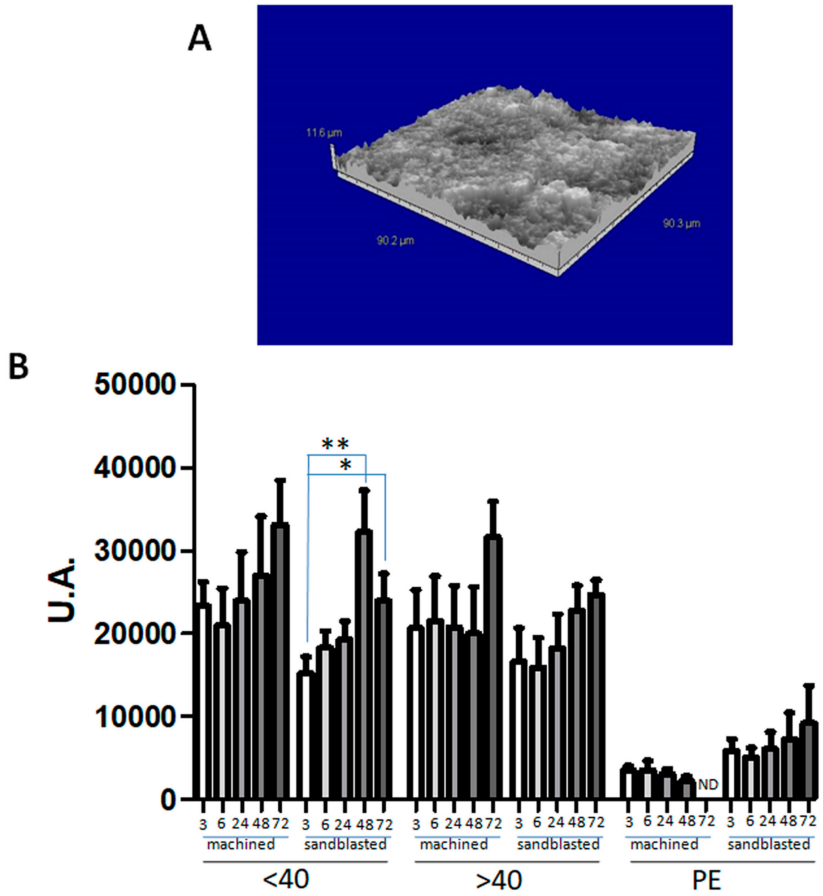

Figure 5. Adhesion of hAMSCs to titanium disks. Panel (**A**) shows a surface view of the sandblasted disk, obtained by the rugosimeter software. Panel (**B**) illustrates the results obtained when CM-DiL-labelled cells (p2) obtained from Group 1 (<40), Group 2 (>40), or Group 3 (PE) were seeded on machined (smooth) or sandblasted titanium disks, and associated fluorescence was assessed at 3, 6, 24, 48, and 72 h. ND: not determined. Results are expressed as mean ± SD of three experiments carried out each in triplicate for each isolate. * $P < 0.05$; ** $P < 0.01$.

This difference reached statistical significance when comparing Group 3 hAMSCs with the corresponding hAMSCs from the other two Groups, at all times and with both types of disks (Table 3). However, the *P*-values were more significant when PE hAMSCs were compared with normal hAMSCs.

Table 3. Differences (*P*-values) of adhesion between Group 3 (PE: pre-eclampsia) vs. Groups 1 (<40) and 2 (>40).

Time/Titanium Disk	Group 1	Group 2
3 h/machined	0.011	0.0358
6 h/machined	0.0049	0.0195
24 h/machined	0.0076	0.0130
48 h/machined	0.0087	0.0246
3 h/sandblasted	0.0013	0.0148
6 h/sandblasted	<0.0001	0.0064
24 h/sandblasted	0.0007	0.0122
48 h/sandblasted	0.0005	0.0716
72 h/sandblasted	0.0199	0.0096

4. Discussion

As MSCs age, their properties gradually become compromised, including the properties of multilineage differentiation, homing, immune modulation, and wound healing [28–30]. Although it is well known that the number and function of BM-MSCs are affected by bone pathology, such as osteoarthritis or osteoporosis [31], no similar studies have been carried out on hAMSCs. In the present study, we have isolated hAMSCs obtained from aged and pre-eclamptic pregnant women accordingly, to established protocols for non-aged hAMSCs [8,9,32,33]. To the best of our knowledge, this is the first time that a comparison of such sources of hAMSCs has been carried out concerning various phenotypic and functional parameters.

Although the yield of hAMSCs from PE donors was lower than that for non-aged and aged women, also these donors gave sufficient numbers of hAMSCs to be expanded and cultured up to passage 5. If, however, we think that the advantage to comply on these ethical sources of MSCs is to yield a higher number of cells and avoid passaging that could lead to karyotypic abnormalities, this is a setback with pathological hAMSCs. Since the gestational age is similar between Group 1 and Group 2, and is even lower in Group 3, how could maternal factors influence the functional behavior of hAMSCs in terms of yield, viability, proliferation, and differentiation? It has been demonstrated that MSCs age in different organs [34], and that the increase in reactive oxygen species and epigenetic changes may underlie these alterations [31,35,36], that may well be at work also in aged placentas. Interestingly, Alrefaei et al. [37] determined by an immunohistochemistry study on MSCs in AM and Warthon's jelly of the umbilical cord, that CD105 and CD29 expression showed an inverse correlation with age, with the least expression in women aged older than 40 years. As concerning pre-eclampsia, this pathological condition is thought to be due to inadequate placental cytotrophoblast invasion, followed by widespread maternal endothelial dysfunction, which leads to placental hypoperfusion and ischemia [38–40]. The only report, to the best of our knowledge, that is concerned about the effects of PE on amniotic cells is the one by Pianta and colleagues [41], who found that surface marker profile of PE-hAMSCs was similar to that of normal hAMSCs, although the expression of co-stimulatory and immunomodulatory molecules was quantitatively different, perhaps as a response to the inflammatory infiltrates that have been detected in the amniotic membranes of pre-eclamptic placentas. Therefore, it is conceivable that alterations in the maternal and placental environment due to ageing and pathology may lead to a dysfunctional behavior (perhaps linked to heightened senescence) in cells belonging to the amniotic membrane, a hypothesis that has to be confirmed with further experiments.

MSCs are characterized by a unique set of membrane molecules involved in adhesion and migration. CD29, which is also known as integrin β1, is highly expressed not only in MSCs but also in macrophages and plays an important role in cell migration [42,43]. CD29 was found to be essential in the trafficking of BM-MSCs to the infarcted myocardium [44]. It is also the principal receptor for binding extracellular matrix (ECM) components, such as laminin, fibronectin, and collagens, and is involved in cell attachment [45]. It has been previously shown that integrin β1 is required for

osteoblastic differentiation on microscale titanium substrates [46]. Slight but significant variations in α3, α4 subunits, and αV expression, as well as β1 and β5 subunits have been observed in the interaction of nanostructured titanium surfaces and MSCs, when studied in terms of focal adhesion and differentiation [47]. Thus, the expression of integrins may condition the spreading and adhesion of MSCs onto titanium surfaces and be in turn affected by attachment to the titanium. Our data strongly indicate that CD29 is implied in adhesion to titanium disks, since PE hAMSCs showed a reduction in both its expression and adhesion, while these features were not affected in hAMSCs obtained from non-aged and aged donors. On the other hand, our data also showed that CD73 (ecto-5′-nucleotidase) was decreased in hAMSCs obtained from aged and PE women. CD73 has been implicated in cell–cell and cell–matrix interactions [48]. However, hAMSCs obtained from aged women did not display a reduction in adhesion to titanium, suggesting that CD73 is not essential for, or contributes at a lower extent, to the adhesion of these cells to titanium. Nevertheless, an interesting relationship between CD29 and CD73 in MSCs has been found. Ode et al. [49] have demonstrated that a mechanical loading of MSCs embedded in fibrin led to a reduced surface expression of CD73 and CD29, but not of CD105, and also to a decrease in the migratory response after loading, possibly via FAK/Src family kinase signaling. Despite the fact that CD29 and CD73 seem to be independently regulated by mechanical loading, nevertheless these results are interesting for a better understanding of the interaction of MSCs with the matrix, and thus their role should be further investigated in the context of adhesion to titanium implants.

Titanium surfaces are increasingly used as the substrate for improving adhesion, osseointegration, and host response in terms of avoiding bacterial contamination [27,50]. Surface roughness has been demonstrated to be an essential parameter to promote osteoblastic differentiation and maturation of MSCs in dental implants made by titanium [4]. In particular, enhanced differentiation and maturation of MSCs towards the osteoblast lineage was shown on sandblasted rough surfaces as compared with smooth surfaces [51–53]. The canonical Wnt signaling is involved in early osteoblast differentiation, $Ca2^{+}$-dependent Wnt5a signaling, as well as Dkk2, BMPs, and integrins, regulates osteoblast differentiation of MSCs on hydrophilic surfaces with hierarchical roughness [4,51]. However, hAMSCs obtained from non-aged and nonpathological pregnancies adhered, survived (and likely initiated to proliferate) similarly on smooth and sandblasted disks. This might be due to the microroughness or other properties of titanium surfaces used in this study, which should be optimized. It has been prospected that increased bone response is obtained when surfaces are modified for their microtopography, surface chemistry, hydrophilicity, and nanoroughness [54].

All in all, our data point out that hAMSCs obtained from aged women can have lower differentiative capacities, but they adhere to the substrate used in osteoinduction and osseointegration as cells from non-aged donors do. On the other hand, PE hAMSCs are not only obtainable with low yield, but also adhere less onto titanium surfaces.

5. Conclusions

In this study, we demonstrated that hAMSCs obtained from pre-eclamptic women are affected in their yield and phenotype as compared with non-aged and nonpathological donors. In particular, a reduced expression of CD29 (a β1 integrin) is accompanied by a detrimental behavior in cell adhesion to titanium surfaces. This study suggests for the first time that amnion as a source of MSCs for osteoinduction and possibly osseointegration of titanium dental implants depends on the presence of pathology.

Supplementary Materials: The following are available online at http://www.mdpi.com/2076-3417/9/17/3471/s1, Figure S1: Morphology of hAMSCs of the three Groups at p0 and p2.

Author Contributions: Conceptualization, M.M. and M.C.; Data curation, M.M., E.B., A.C., D.L., A.A. and M.C.; Formal analysis, M.C.; Investigation, E.B., A.C., S.C. and S.D.G.; Methodology, E.B., A.C., S.C., L.M. and S.D.G.; Writing—original draft, M.C.; Writing—review & editing, M.M., L.M., D.L. and M.C.

Funding: This research received no external funding.

Acknowledgments: We thank Teresa Nittoli for her valuable technical assistance and expertise, Titanmed SRL (Trezzano sul Naviglio, Milan, Italy) for having provided us with the 3D image of sandblasted disk, and Carmine Di Mario for proofreading the manuscript.

Conflicts of Interest: The authors declare no conflict of interest.

References

1. Mao, X.; Liu, Y.; Chen, C.; Shi, S. Mesenchymal Stem Cells and Their Role in Dental Medicine. *Dent. Clin. North. Am.* **2017**, *61*, 161–172. [CrossRef] [PubMed]
2. Egusa, H.; Sonoyama, W.; Nishimura, M.; Atsuta, I.; Akiyama, K. Stem cells in dentistry—Part II: Clinical applications. *J. Prosthodont. Res.* **2012**, *56*, 229–248. [CrossRef] [PubMed]
3. LeGeros, R.Z. Calcium Phosphate-Based Osteoinductive Materials. *Chem. Rev.* **2008**, *108*, 4742–4753. [CrossRef] [PubMed]
4. Olivares-Navarrete, R.; Hyzy, S.L.; Hutton, D.L.; Erdman, C.P.; Wieland, M.; Boyan, B.D.; Schwartz, Z. Direct and Indirect Effects of Microstructured Titanium Substrates on the Induction of Mesenchymal Stem Cell Differentiation towards the Osteoblast Lineage. *BioMat.* **2010**, *31*, 2728–2735. [CrossRef] [PubMed]
5. Egusa, H.; Sonoyama, W.; Nishimura, M.; Atsuta, I.; Akiyama, K. Stem cells in dentistry—Part I: Stem cell sources. *J. Prosthodont. Res.* **2012**, *56*, 151–165. [CrossRef] [PubMed]
6. Toda, A.; Okabe, M.; Yoshida, T.; Nikaido, T. The potential of amniotic membrane/amnion-derived cells for regeneration of various tissues. *J. Pharmacol. Sci.* **2007**, *105*, 215–228. [CrossRef] [PubMed]
7. Parolini, O.; Alviano, F.; Bagnara, G.P.; Bilic, G.; Buhring, H.J.; Evangelista, M.; Hennerbichler, S.; Liu, B.; Magatti, M.; Mao, N.; et al. Concise review: Isolation and characterization of cells from human term placenta: Outcome of the first international Workshop on Placenta Derived Stem Cells. *Stem Cells* **2008**, *26*, 300–311. [CrossRef] [PubMed]
8. Portmann-Lanz, C.B.; Schoeberlein, A.; Huber, A.; Sager, R.; Malek, A.; Holzgreve, W.; Surbek, D.V. Placental mesenchymal stem cells as potential autologous graft for pre- and perinatal neuroregeneration. *Am. J. Obstet. Gynecol.* **2006**, *194*, 664–673. [CrossRef]
9. Alviano, F.; Fossati, V.; Marchionni, C.; Arpinati, M.; Bonsi, L.; Franchina, M.; Lanzoni, G.; Cantoni, S.; Cavallini, C.; Bianchi, F.; et al. Term amniotic membrane is a high throughput source for multipotent mesenchymal stem cells with the ability to differentiate into endothelial cells in vitro. *BMC Dev. Boil.* **2007**, *7*, 11.
10. Soncini, M.; Vertua, E.; Gibelli, L.; Zorzi, F.; Denegri, M.; Albertini, A.; Wengler, G.S.; Parolini, O. Isolation and characterization of mesenchymal cells from human fetal membranes. *J. Tissue Eng. Regen. Med.* **2007**, *1*, 296–305. [CrossRef]
11. Manuelpillai, U.; Moodley, Y.; Borlongan, C.; Parolini, O.; Borlongan, C. Amniotic membrane and amniotic cells: Potential therapeutic tools to combat tissue inflammation and fibrosis? *Placenta* **2011**, *32*, S320–S325. [CrossRef]
12. Rennie, K.; Gruslin, A.; Hengstschläger, M.; Pei, D.; Cai, J.; Nikaido, T.; Bani-Yaghoub, M. Applications of Amniotic Membrane and Fluid in Stem Cell Biology and Regenerative Medicine. *Stem Cells Int.* **2012**, *2012*, 1–13. [CrossRef]
13. Carbone, A.; Paracchini, V.; Castellani, S.; Gioia, S.; Seia, M.; Colombo, C.; Conese, M. Human Amnion-Derived Cells: Prospects for the Treatment of Lung Diseases. *Curr. Stem Cell Res. Ther.* **2014**, *9*, 297–305. [CrossRef]
14. Kmiecik, G.; Spoldi, V.; Silini, A.; Parolini, O. Current View on Osteogenic Differentiation Potential of Mesenchymal Stromal Cells Derived from Placental Tissues. *Stem. Cell. Rev.* **2015**, *11*, 570–585. [CrossRef]
15. Caplan, A. Why are MSCs therapeutic? New data: New insight. *J. Pathol.* **2009**, *217*, 318–324. [CrossRef]
16. Stolzing, A.; Jones, E.; McGonagle, D.; Scutt, A. Age-related changes in human bone marrow-derived mesenchymal stem cells: Consequences for cell therapies. *Mech. Ageing Dev.* **2008**, *129*, 163–173. [CrossRef]
17. Zhou, S.; Greenberger, J.S.; Epperly, M.W.; Goff, J.P.; Adler, C.; LeBoff, M.S.; Glowacki, J. Age-Related Intrinsic Changes in Human Bone Marrow-Derived Mesenchymal Stem Cells and Their Differentiation to Osteoblasts. *Aging Cell* **2008**, *7*, 335–343. [CrossRef]
18. D'Ippolito, G.; Schiller, P.C.; Ricordi, C.; Roos, B.A.; Howard, G.A. Age-Related Osteogenic Potential of Mesenchymal Stromal Stem Cells from Human Vertebral Bone Marrow. *J. Bone Miner. Res.* **1999**, *14*, 1115–1122. [CrossRef]

19. Scheubel, R.J.; Zorn, H.; Silber, R.-E.; Kuss, O.; Morawietz, H.; Holtz, J.; Simm, A. Age-dependent depression in circulating endothelial progenitor cells in patients undergoing coronary artery bypass grafting. *J. Am. Coll. Cardiol.* **2003**, *42*, 2073–2080. [CrossRef]
20. Heeschen, C.; Lehmann, R.; Honold, J.; Assmus, B.; Aicher, A.; Walter, D.H.; Martin, H.; Zeiher, A.M.; Dimmeler, S.; Oudit, G.Y.; et al. Profoundly Reduced Neovascularization Capacity of Bone Marrow Mononuclear Cells Derived From Patients With Chronic Ischemic Heart Disease. *Circulation* **2004**, *109*, 1615–1622. [CrossRef]
21. Powe, C.E.; Levine, R.J.; Karumanchi, S.A. Preeclampsia, a disease of the maternal endothelium: The role of anti-angiogenic factors and implications for later cardiovascular disease. *Circulation* **2011**, *123*, 2856–2869. [CrossRef]
22. Banek, C.T.; Gilbert, J.S. Approaching the threshold for predicting preeclampsia: Monitoring angiogenic balance during pregnancy. *Hypertension* **2011**, *58*, 774–775. [CrossRef]
23. Nelson, D.M.; Burton, G.J. A technical note to improve the reporting of studies of the human placenta. *Placenta* **2011**, *32*, 195–196. [CrossRef]
24. American College of Obstetricians and Gynecologists. Hypertension in pregnancy. Report of the American College of Obstetricians and Gynecologists' Task Force on Hypertension in Pregnancy. *Obstet. Gynecol.* **2013**, *122*, 1122–1131.
25. Paracchini, V.; Carbone, A.; Colombo, F.S.; Castellani, S.; Mazzucchelli, S.; Di Gioia, S.; DeGiorgio, D.; Seia, M.; Porretti, L.; Colombo, C.; et al. Amniotic Mesenchymal Stem Cells: A New Source for Hepatocyte-Like Cells and Induction of CFTR Expression by Coculture with Cystic Fibrosis Airway Epithelial Cells. *J. Biomed. Biotechnol.* **2012**, *2012*, 1–15. [CrossRef]
26. Carbone, A.; Valente, M.; Annacontini, L.; Castellani, S.; Di Gioia, S.; Parisi, D.; Rucci, M.; Belgiovine, G.; Colombo, C.; Di Benedetto, A.; et al. Adipose-derived mesenchymal stromal (stem) cells differentiate to osteoblast and chondroblast lineages upon incubation with conditioned media from dental pulp stem cell-derived osteoblasts and auricle cartilage chondrocytes. *J. Boil. Regul. Homeost. Agents* **2016**, *30*, 111–122.
27. Lepore, S.; Milillo, L.; Trotta, T.; Castellani, S.; Porro, C.; Panaro, M.A.; Santarelli, A.; Bambini, F.; Muzio, L.L.; Conese, M.; et al. Adhesion and growth of osteoblast-like cells on laser-engineered porous titanium surface: Expression and localization of N-cadherin and beta-catenin. *J. Boil. Regul. Homeost. Agents* **2013**, *27*, 531–541.
28. Yu, K.R.; Kang, K.S. Aging-Related Genes in Mesenchymal Stem Cells: A Mini-Review. *Gerontology* **2013**, *59*, 557–563. [CrossRef]
29. Block, T.J.; Marinkovic, M.; Tran, O.N.; Gonzalez, A.O.; Marshall, A.; Dean, D.D.; Chen, X.D. Restoring the quantity and quality of elderly human mesenchymal stem cells for autologous cell-based therapies. *Stem Cell Res. Ther.* **2017**, *8*, 239. [CrossRef]
30. Mueller, S.M.; Glowacki, J. Age-related decline in the osteogenic potential of human bone marrow cells cultured in three-dimensional collagen sponges. *J. Cell. Biochem.* **2001**, *82*, 583–590. [CrossRef]
31. Ganguly, P.; El-Jawhari, J.; Ponchel, F. age related changes in bone marrow mesenchymal stromal cells: a potential impact on osteoporosis and osteoarthritis development. *Cell Transplant.* **2017**, *26*, 1520–1529. [CrossRef]
32. Moore, R.; Silver, R.; Moore, J. Physiological Apoptotic Agents have Different Effects upon Human Amnion Epithelial and Mesenchymal Cells. *Placenta* **2003**, *24*, 173–180. [CrossRef]
33. Zhao, P.; Ise, H.; Hongo, M.; Ota, M.; Konishi, I.; Nikaido, T. Human amniotic mesenchymal cells have some characteristics of cardiomyocytes. *Transplantation* **2005**, *79*, 528–535. [CrossRef]
34. Liu, H.; Xia, X.; Li, B. Mesenchymal stem cell aging: Mechanisms and influences on skeletal and non-skeletal tissues. *Exp. Boil. Med.* **2015**, *240*, 1099–1106. [CrossRef]
35. Khan, H.; Mafi, P.; Mafi, R.; Khan, W. The Effects of Ageing on Differentiation and Characterisation of Human Mesenchymal Stem Cells. *Curr. Stem. Cell. Res. Ther.* **2018**, *13*, 378–383. [CrossRef]
36. Li, Y.; Wu, Q.; Wang, Y.; Li, L.; Bu, H.; Bao, J. Senescence of mesenchymal stem cells. *Int. J. Mol. Med.* **2017**, *39*, 775–782. [CrossRef]
37. Alrefaei, G.I.; Ayuob, N.N.; Ali, S.S.; Al-Karim, S. Effects of maternal age on the expression of mesenchymal stem cell markers in the components of human umbilical cord. *Folia Histochem. Cytobiol.* **2015**, *53*, 259–271. [CrossRef]
38. Young, B.C.; Levine, R.J.; Karumanchi, S.A. Pathogenesis of preeclampsia. *Annu. Rev. Pathol.* **2010**, *5*, 173–192. [CrossRef]

39. Gathiram, P.; Moodley, J. Pre-eclampsia: Its pathogenesis and pathophysiolgy. *Cardiovasc. J. Afr.* **2016**, *27*, 71–78. [CrossRef]
40. Phipps, E.; Prasanna, D.; Brima, W.; Jim, B. Preeclampsia: Updates in Pathogenesis, Definitions, and Guidelines. *Clin. J. Am. Soc. Nephrol.* **2016**, *11*, 1102–1113. [CrossRef]
41. Pianta, S.; Magatti, M.; Vertua, E.; Bonassi Signoroni, P.; Muradore, I.; Nuzzo, A.M.; Rolfo, A.; Silini, A.; Quaglia, F.; Todros, T.; et al. Amniotic mesenchymal cells from pre-eclamptic placentae maintain immunomodulatory features as healthy controls. *J. Cell. Mol. Med.* **2016**, *20*, 157–169. [CrossRef]
42. Miao, L.; Xin, X.; Xin, H.; Shen, X.; Zhu, Y.Z. Hydrogen Sulfide Recruits Macrophage Migration by Integrin beta1-Src-FAK/Pyk2-Rac Pathway in Myocardial Infarction. *Sci. Rep.* **2016**, *6*, 22363. [CrossRef]
43. Suto, E.G.; Mabuchi, Y.; Suzuki, N.; Suzuki, K.; Ogata, Y.; Taguchi, M.; Muneta, T.; Sekiya, I.; Akazawa, C. Prospectively isolated mesenchymal stem/stromal cells are enriched in the $CD73^{+}$ population and exhibit efficacy after transplantation. *Sci. Rep.* **2017**, *7*, 4838. [CrossRef]
44. Ip, J.E.; Wu, Y.; Huang, J.; Zhang, L.; Pratt, R.E.; Dzau, V.J. Mesenchymal stem cells use integrin beta1 not CXC chemokine receptor 4 for myocardial migration and engraftment. *Mol. Biol. Cell.* **2007**, *18*, 2873–2882. [CrossRef]
45. Pytela, R.; Pierschbacher, M.D.; Ruoslahti, E. Identification and isolation of a 140 kd cell surface glycoprotein with properties expected of a fibronectin receptor. *Cell* **1985**, *40*, 191–198. [CrossRef]
46. Olivares-Navarrete, R.; Raz, P.; Zhao, G.; Chen, J.; Wieland, M.; Cochran, D.L.; Chaudhri, R.A.; Ornoy, A.; Boyan, B.D.; Schwartz, Z. Integrin alpha2beta1 plays a critical role in osteoblast response to micron-scale surface structure and surface energy of titanium substrates. *Proc. Natl. Acad. Sci. USA* **2008**, *105*, 15767–15772. [CrossRef]
47. Lavenus, S.; Berreur, M.; Trichet, V.; Pilet, P.; Louarn, G.; Layrolle, P. Adhesion and osteogenic differentiation of human mesenchymal stem cells on titanium nanopores. *Eur. Cell. Mater* **2011**, *22*, 84–96. [CrossRef]
48. Zimmermann, H. 5′-Nucleotidase: Molecular structure and functional aspects. *Biochem. J.* **1992**, *285*, 345–365. [CrossRef]
49. Ode, A.; Kopf, J.; Kurtz, A.; Schmidt-Bleek, K.; Schrade, P.; Kolar, P.; Buttgereit, F.; Lehmann, K.; Hutmacher, D.W.; Duda, G.N.; et al. CD73 and CD29 concurrently mediate the mechanically induced decrease of migratory capacity of mesenchymal stromal cells. *Eur. Cell. Mater.* **2011**, *22*, 26–42. [CrossRef]
50. Spriano, S.; Yamaguchi, S.; Baino, F.; Ferraris, S. A critical review of multifunctional titanium surfaces: New frontiers for improving osseointegration and host response, avoiding bacteria contamination. *Acta Biomater.* **2018**, *79*, 1–22. [CrossRef]
51. Olivares-Navarrete, R.; Hyzy, S.L.; Park, J.H.; Dunn, G.R.; Haithcock, D.A.; Wasilewski, C.E.; Boyan, B.D.; Schwartz, Z. Mediation of osteogenic differentiation of human mesenchymal stem cells on titanium surfaces by a Wnt-integrin feedback loop. *Biomaterials* **2011**, *32*, 6399–6411. [CrossRef]
52. Gittens, R.A.; Olivares-Navarrete, R.; Cheng, A.; Anderson, D.M.; McLachlan, T.; Stephan, I.; Geis-Gerstorfer, J.; Sandhage, K.H.; Fedorov, A.G.; Rupp, F.; et al. The roles of titanium surface micro/nanotopography and wettability on the differential response of human osteoblast lineage cells. *Acta Biomater.* **2013**, *9*, 6268–6277. [CrossRef]
53. Boyan, B.; Cheng, A.; Olivares-Navarrete, R.; Schwartz, Z. Implant Surface Design Regulates Mesenchymal Stem Cell Differentiation and Maturation. *Adv. Dent. Res.* **2016**, *28*, 10–17. [CrossRef]
54. Wennerberg, A.; Albrektsson, T. On implant surfaces: A review of current knowledge and opinions. *Int. J. Oral Maxillofac. Implant.* **2010**, *25*, 63–74.

© 2019 by the authors. Licensee MDPI, Basel, Switzerland. This article is an open access article distributed under the terms and conditions of the Creative Commons Attribution (CC BY) license (http://creativecommons.org/licenses/by/4.0/).